Comparison of Prefabricated Cage System with Existing Reinforcement Methods in Concrete Columns

A Thesis

Presented in Partial Fulfillment of the Requirements for

Graduation with Distinction with the Degree Bachelor of Science

in the Civil Engineering Department of the

College of Engineering of The Ohio State University

By

Matthew John Fisher

*****

The Ohio State University

2006

Undergraduate Honors Examination Committee:

Dr. Halil Sezen, Advisor

Dr. Shive Chaturvedi

Approved by:

____

Advisor

Civil Engineering Honors Undergraduate Program

ABSTRACT

A reinforced concrete column is composed of two main load bearing mechanisms; concrete and a steel reinforcing cage. The concrete is the primary vertical load bearing mechanism with the steel cage providing some vertical load carrying capacity while serving mainly to confine the core concrete. The steel cage consists of two types of bars; longitudinal, which carry any compressive or tensile loads, and transverse, which hold the longitudinal bars in place and also provide confinement of the core concrete under axial load. The transverse bars are bent and tied to the longitudinal bars.

A new type of steel cage has recently been proposed by Halil Sezen PhD and Mohammad Shamsai PhD, both of The Ohio State University. The new method is termed Prefabricated Cage System (PCS) reinforcement, and it consists of a cage constructed from a solid steel tube. A grid is cut into the tube through the use of a laser-cutter, resulting in a reinforcing cage that is very similar to a rebar cage. The main differences between the two are: 1) The PCS cage is a solid entity, while the rebar cage is held together through the use of ties. 2) The steel in the PCS cage is in rectangular form while the steel in the rebar cage typically consists of round bars. The machine fabrication of PCS provides a more accurately constructed column, compared to the manually constructed rebar cage, at the same or less cost than a rebar column due to the reduced on-site construction time required by PCS.

The research project will focus on the performance of PCS in circular columns. In all, six

samples will be constructed and tested, consisting of two rebar reinforced columns and four PCS reinforced columns. Each test column will be 18 in. in height with a 6 in. diameter. There will be two test groups, each group containing one rebar column and two PCS columns. The strength of the steel, which is represented by the yield stress of the steel multiplied by the cross-sectional area of the steel, will be the same in each test group to allow for accurate comparisons.

The purpose of this research is to not only compare the performance of a PCS reinforced column to a rebar reinforced column, but also to compare PCS cages with differently sized grid openings. The objective is to investigate whether the PCS column has a higher maximum load and a larger displacement capacity, due to the increased confinement provided by the rectangular shape of the PCS cage over the round shape of the rebar cage.

TABLE OF CONTENTS

LIST OF TABLES

LIST OF FIGURES

CHAPTER 1

INTRODUCTION

1.1 Introduction

Reinforced concrete, a composite material consisting of steel and concrete, is commonly used in the construction of buildings and other structures, and has been for many decades. Concrete, by itself, is very strong in compression but very weak in tension. Steel is strong in both tension and compression. The benefit from concrete comes from its relatively low cost compared to steel. When a small amount of steel is added to a concrete member in the tension zone, the result is a load bearing member that is strong in both tension and compression. While reinforced concrete is used in the construction of a variety of different structural members, such as shear walls, footings, beams and retaining walls, one of its most common applications is in the construction of columns. The application of reinforced concrete in circular columns will be examined in this research project.

1.2 Reinforcement Systems

There is a variety of reinforcement methods currently used in the field, with rebar cages being the most commonly utilized method. Other methods include welded wire fabric (WWF) and concrete-filled tubes (CFT). Recently an alternative method, known as prefabricated cage system (PCS) reinforcement, has recently been proposed (Shamsai 2006). For the purpose of this research project only two methods, rebar and PCS, will be analyzed and compared.

1.2.1 Rebar Reinforcement System

In a traditional reinforced concrete column, a reinforcing cage is formed using steel bars known as rebar. The cage consists of two types of bars; longitudinal, which carry any compressive or tensile loads, and transverse, which serve to confine the concrete inside of the reinforcement, known as the core concrete. The core concrete and longitudinal steel are the main bearers of the compressive load in a reinforced concrete column. The transverse bars are bent so that they fit around the longitudinal bars, and then tied into place.

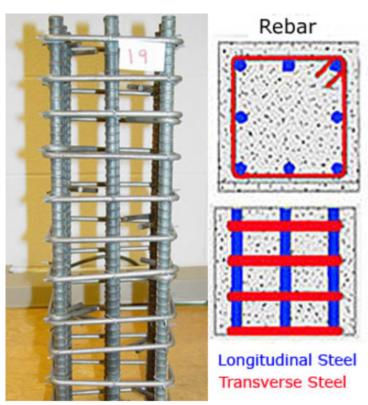

Figure 1.1 – Rebar reinforcement system

1.2.2 Prefabricated Cage System (PCS) Reinforcement

Recently, a new method of steel reinforcement has been proposed by Sezen PhD and Shamsai PhD, both from Ohio State University. Prefabricated Cage System (PCS) reinforcement is a monolithic reinforcing cage constructed from a hollow steel tube. A grid is cut into the tube through the use of a laser, resulting in a reinforcing cage that is very similar to a rebar cage. An example of a square PCS column is shown in Figure 1.2.

Figure 1.2 – Square PCS reinforcement (Shamsai 2006)

1.2.3 Production

Rebar cages consist of individual reinforcing bars and transverse ties. The bars come pre-bent to the site specifications, but are not preassembled in any way. The cages are assembled on-site by attaching the transverse hoops or spirals to the longitudinal bars with small steel ties. The ties are twisted around the bars to hold them in place. This is a labor intensive process and can result in inaccuracies during assembly. PCS is created through the use of a laser-cutter in a machine shop. The laser-cutter is controlled by a computer, with accuracies to within 0.1 to 0.01 in. This allows for a reinforcing cage with final dimensions that are much closer to the specified dimensions.

1.2.4 Construction Time

As was previously discussed, the field construction of rebar cages is a time and labor intensive process. Each transverse hoop or spiral must be tied to the longitudinal bars. For example, a column that is 8 ft tall with 12 longitudinal bars and a transverse spacing of 4 in. would require a total of 144 ties, if every other bar is skipped in the tying process. PCS, on the other hand, comes prefabricated to the job site, requiring significantly less time and labor to set into place. Many construction projects have very strict deadlines, with some bridge replacements needing to be completed in a matter of days to avoid excessive traffic delays. Using PCS instead of rebar cages would save hours of labor that would have been spent tying the rebar cages, resulting in the project being finished in a shorter period of time.

1.2.5 Cost

Shamsai (2006) conducted an economic analysis of PCS and rebar columns. The initial cost of fabrication for PCS is currently greater than rebar due to the high cost of laser-cutting. However, rebar cages must be assembled on-site, making their construction more labor-intensive and thus more expensive. The conclusion reached by Shamsai was that the total overall cost of a PCS column, including fabrication and labor, was approximately 7% less than that of a similar rebar column. The cost of PCS columns would further decrease if it were to become mass produced, which would result in a decrease in fabrication cost.

1.3 Project Scope

Two steel reinforcement methods, rebar and PCS, are to be analyzed through the testing of small-scale columns. The test columns are to be loaded under axial load to failure at a constant rate of approximately 0.004 in. / sec. The axial load versus deflection performance for each column will be recorded. Certain responses throughout the testing process will be marked, such as the first appearance of cracking, spalling of the cover concrete, yielding of the steel reinforcement and fracture of the transverse reinforcement. The behavior of the PCS reinforced columns will be compared to the behavior of the rebar reinforced columns, in order to determine the advantages and disadvantages of each method.

1.4 Objectives

The proposed project will focus on further testing and development of PCS reinforcement. The two main variables in PCS reinforcement are the thickness of the steel tube and the dimensions of the openings in the grid. There are a wide range of possibilities that can result in the same steel yielding force, which is defined as the cross-sectional area of steel multiplied by the yield strength of the steel. This project will consist of two test groups, each group pairing two PCS samples with one rebar sample. The samples within the group will all have the same steel yield force. The two groups will have different steel yield forces.

The research project has one main objective and two other secondary objectives. The main objective of this research project is to compare analytically the strength and ductility of the PCS columns within a group to the corresponding rebar column to determine how the strength of PCS reinforcement compares to rebar reinforcement of equal cross-sectional areas of steel. The secondary objectives of this research project are to compare the performance of each PCS column within a group to determine if one combination of wall thickness and grid opening size is stronger than the other, and to compare the PCS columns from the two different groups to determine if one steel yield force performs better than another, taking into account the added strength that a larger steel yield force provides.

1.5 Project Summary

A total of six columns are designed for testing, consisting of two rebar reinforced columns and four PCS reinforced columns. The specimens are split into two groups, with each member in a group having the same steel yield force. The materials to be used in construction of the test columns have all been acquired and tested according to ASTM standards in order to develop an accurate understanding of the mechanical properties of the materials. The mechanical properties of the materials are then modeled in order to construct a theoretical axial load-deflection model for each test column.

Construction of the test columns was delayed during the laser-cutting of the steel tubes phase. A total of 25 laser-cutting manufacturers throughout Ohio were contacted, with a majority of the companies either unable to manufacture the column or unavailable for six weeks or longer. The disinterest of many of the companies was most likely due to the insignificant profit offered by such a small order of only four tubes. Only two companies provided estimates, with one company submitting an estimate of $3000 for cutting the four tubes and the other submitting an estimate of $1000 for the four columns. Both estimates exceeded the project budget. This project is expected to be completed as part of a larger Masters Thesis research project next year. Once the tubes are laser-cut, construction of the test columns will be possible. The actual test columns will be constructed and tested in order to determine the actual loading characteristics of the test columns. The actual data will be compared to the theoretical models in order to better understand the performance of the reinforcement methods.

To this point, the materials for the research project have been obtained and tested in order to determine their mechanical properties, and the rebar cages have been constructed. The mechanical properties of these materials were modeled using existing equations in order to incorporate them into theoretical models. Two different concrete confinement models were studied and used to construct theoretical axial load-deflection diagrams for all six columns. These diagrams show the expected results for each column. They will later be compared to the actual test results in order to better understand the performance of PCS compared to rebar reinforcement.

CHAPTER 2

CONFINED CONCRETE MODELS

2.1 Introduction

Much research has been conducted in an attempt to model the performance of reinforced concrete columns under axial load. Because it is a composite material, its true behavior is very difficult to model. Both materials, concrete and steel, behave non-linearly and are modeled using a piece-wise stress-strain performance curve, making modeling of these materials fairly difficult. This chapter briefly discusses the models of the materials and the methods used to obtain them. A more detailed description of the equations used in the models can be found in Chapter 4.

2.1.1 Plain Concrete Behavior

Typically, the behavior of plain concrete is obtained by testing 8 cylinders, having a height of 12 in. and a diameter of 6 in., at 28 days after casting. The peak value obtained from these tests is said to be the ultimate compressive strength and is denoted as f'_c. The standard stress vs. strain plot for plain concrete begins in a parabolic shape up until the ultimate strength, at which point the strength declines linearly until failure, as shown in Figure 2.1.

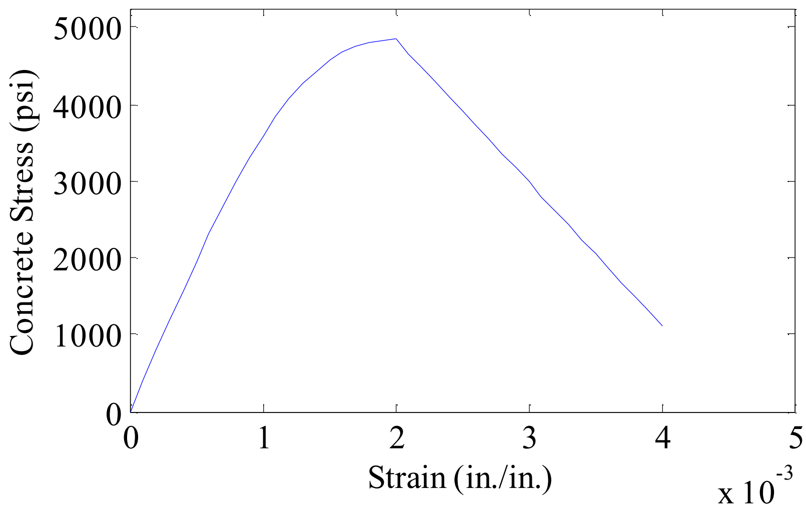

Figure 2.1 – Typical stress vs. strain plot for plain concrete

2.1.2 Steel Behavior

As with concrete, the behavior of steel is determined through testing. Small samples, coupons, of the steel must be constructed according to ASTM standards. The coupons are then loaded under tension until fracture, with an extensometer used to measure the strain in the coupon. The critical sections in the steel stress-strain plot are the yield stress and strain (f_y and ε_y), the modulus of elasticity (E_s), the ultimate stress (f_u) and the rupture strain (ε_r). The data obtained from this test will allow the steel to be modeled. The stress versus strain plot for steel is composed of three different phases, beginning with the linear elastic phase up until the yield strength, then transitioning into strain hardening up to the ultimate strength, followed by necking and fracture, as shown in Figure 2.2 below.

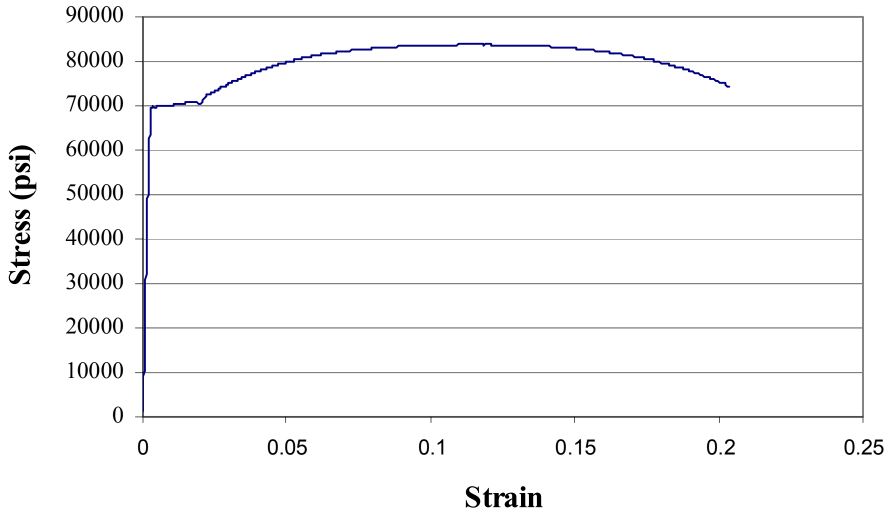

Figure 2.2 – Typical stress versus strain plot for steel rebar

2.2 Confinement

As a concrete column is compressed, the axial stress causes the concrete to expand outwards. Without any type of confinement, the concrete would continue to expand outwards until failure, as seen in the cylinder tests. Research has shown that the strength of a concrete column can be greatly increased through confinement by steel bars (Mander et al. 1988). The steel bars create a confining stress on the core concrete. Once the concrete reaches its non-reinforced crushing strain, typically 0.003 in. / in., the cover concrete will break away and spall off of the column, exposing the steel reinforcing bars and the core concrete. Spalling is then followed by a process referred to as arching, where the concrete between the ties crushes out to form an arch shape (Mander et al. 1988). Figure 2.3, in section A-A, shows an example of arching in a confined concrete column. The arch that is formed then serves to exert a greater confining stress on the core concrete, due to the strong compressive nature of an arch. This process serves to further reinforce the column, greatly increasing its overall strength and ductility.

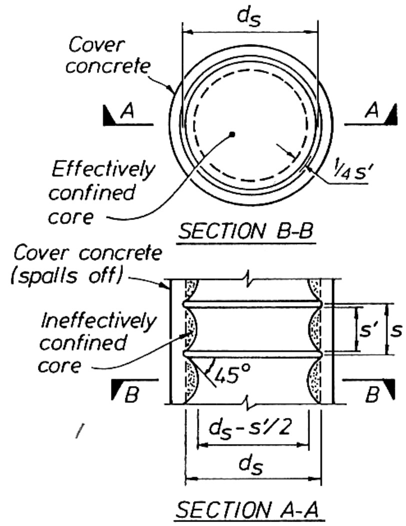

Figure 2.3 – Effectively confined core for circular hoop reinforcement

(Mander et al. 1988)

Research has also shown that confinement can be improved by decreasing the spacing between ties, increasing the ratio of transverse reinforcement to volume of the concrete core, or by using spiral reinforcement instead of ties (Mander et al. 1988). Not only does confining the concrete allow for a greater overall compressive strength of a column, but it greatly increases the ductility of the column as well. This allows the column to absorb a much greater amount of energy before ultimately failing. Ductile failure is also a much more desired form of failure because of the increased amount of warning that it provides over a much more sudden brittle failure. An example of effectively confined concrete core is shown in Figure 2.3 above.

2.3 Confinement Models

For the purpose of this project, the confined concrete models proposed by Mander et al. (1988) and Hoshikuma et al. (1997) will be examined and used for modeling the experimental columns.

2.3.1 Mander et al. Model

The confined concrete model proposed by Mander et al. is one of the most well known and commonly used models. A diagram of Mander et al.'s model, representing unconfined and confined concrete, is shown in Figure 2.4.

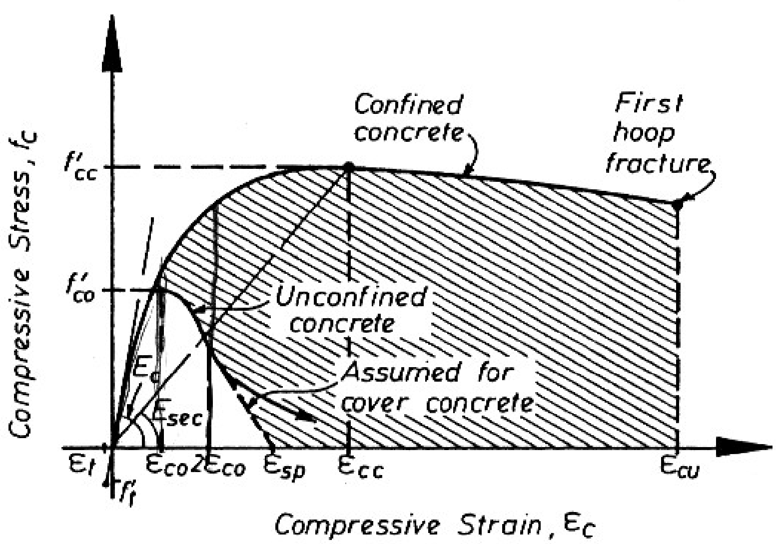

Figure 2.4 – Stress-Strain model proposed for monotonic loading of confined and unconfined concrete (Mander et al. 1988)

Equation 2.1 is used to model the behavior of the confined concrete.

$$f_c = \frac{f'_{cc}\, xr}{r - 1 + x^r} \qquad 2.1$$

The value of the variable x is defined in Equation 2.2, with ε_c being the strain in the concrete and ε_{cc} the strain corresponding to the ultimate confined concrete stress, f'_{cc}. The value of ε_{cc} is defined in equation 2.3, with the value of f'_{cc} defined later on in equation 2.11, f'_{co} being the compressive strength of the unconfined concrete and the value of ε_{co} generally accepted to be .002. The variable r is defined in Equation 2.4 as a function of the modulus of elasticity, E_c, and the secant modulus of elasticity of concrete, E_{sec}, which are defined in Equations 2.5 and 2.6, respectively.

$$x = \frac{\varepsilon_c}{\varepsilon_{cc}} \qquad 2.2$$

$$\varepsilon_{cc} = \varepsilon_{co}\left[1 + 5\left(\frac{f'_{cc}}{f'_{co}} - 1\right)\right] \qquad 2.3$$

$$r = \frac{E_c}{E_c - E_{\sec}} \qquad 2.4$$

$$E_c = 5000\sqrt{f'_{co}}\,(MPa) \qquad 2.5$$

$$E_{\sec} = \frac{f'_{cc}}{\varepsilon_{cc}} \qquad 2.6$$

The confinement effectiveness coefficient, k_e, is defined in Equation 2.7 for spiral transverse reinforcement and in Equation 2.8 for circular hoop transverse reinforcement.

$$k_e = \frac{1 - \frac{s'}{2d_s}}{1 - \rho_{cc}} \qquad 2.7$$

$$k_e = \frac{\left(1 - \frac{s'}{2d_s}\right)^2}{1 - \rho_{cc}} \qquad 2.8$$

The variable s' is equal to the clear spacing between transverse hoops, d_s is equal to the diameter of the transverse reinforcement, as shown in Figure 2.3, and ρ_{cc} is equal to the ratio of the area of longitudinal steel reinforcement to the area of core concrete. The variable ρ_s is defined in Equation 2.9, and is equal to the ratio of the volume of transverse confining steel to the volume of confined concrete core.

$$\rho_s = \frac{4A_{sp}}{d_s s} \qquad 2.9$$

where A_{sp} is equal to the cross-sectional area of transverse reinforcement and s is equal to the center-to-center spacing of the transverse reinforcement. The equation for the effective lateral confining stress on the concrete, f'_l, is defined in Equation 2.10, with f_{yh} being the yield strength of the transverse reinforcement.

$$f'_l = \frac{1}{2} k_e \rho_s f_{yh} \qquad 2.10$$

Once the effective lateral confining stress on the concrete has been calculated, it is possible to calculate the ultimate confined compressive strength of the concrete column, f'_{cc}, through Equation 2.11.

$$f'_{cc} = f'_{co}\left(-1.254 + 2.254\sqrt{1+\frac{7.94 f'_l}{f'_{co}}} - 2\frac{f'_l}{f'_{co}}\right) \qquad 2.11$$

With the ultimate confined concrete stress calculated, the stress-strain relationship for the column can be calculated through the use of Equation 2.1. According to Mander et al. (1988), column failure occurs at the first transverse reinforcement fracture. After this fracture there is a sudden decrease in load capacity. A common estimate for the strain at which the first hoop failure occurs is 0.05, and this value will be used for modeling the columns in this research project.

2.3.2 Hoshikuma et al.

Unlike the model proposed by Mander et al., the model proposed by Hoshikuma et al. consists of two separate equations, one for the ascending branch and one for the descending branch. The ascending branch is defined by Equation 2.12.

$$f_c = E_c \varepsilon_c \left[1 - \frac{1}{n}\left(\frac{\varepsilon_c}{\varepsilon_{cc}}\right)^{n-1}\right] \qquad 2.12$$

The variable *n* is defined by Equation 2.13 as a function of the modulus of elasticity, the ultimate confined concrete strength and the corresponding ultimate strain.

$$n = \frac{E_c \varepsilon_{cc}}{E_c \varepsilon_{cc} - f'_{cc}} \qquad 2.13$$

The descending branch of the stress-strain curve is defined in Equation 2.14.

$$f_c = f'_{cc} - E_{des}\left(\varepsilon_c - \varepsilon_{cc}\right) \qquad 2.14$$

where f'_{cc} is the ultimate compressive strength of the confined concrete and E_{des} is the deterioration rate, which is defined in Equation 2.15.

$$E_{des} = \frac{11.2}{\left(\rho_s f_{yh} \big/ f^2{}_{co}\right)} \qquad 2.15$$

where ρ_s is the volumetric steel ratio, f_{yh} is the transverse steel yield strength, and f_{co} is the ultimate compressive strength of the unconfined concrete. The ultimate compressive strength of the confined core concrete, f'_{cc}, is defined by Equation 2.16, while Equation 2.17 defines the equation used to calculate ε_{cc}.

$$f'_{cc} = f_{co}\left(1.0 + 3.83\left(\frac{\rho_s f_{yh}}{f_{co}}\right)\right) \qquad 2.16$$

$$\varepsilon_{cc} = 0.00218 + 0.0332\left(\frac{\rho_s f_{yh}}{f_{co}}\right) \qquad 2.17$$

The ultimate strain of the column is defined by Equation 2.18

$$\varepsilon_{cu} = \varepsilon_{cc} + \frac{f'_{cc}}{2E_{des}} \qquad 2.18$$

CHAPTER 3

EXPERIMENTAL DESIGN

3.1 Introduction

A total of six columns are to be constructed and tested to investigate the performance of PCS reinforcement in circular columns. Two rebar columns will be used as the control for each group, with the PCS columns being compared to the control columns. The dimensioning and design of each column was based off of the measured steel material properties, and this process will be discussed in this chapter.

Previous research on PCS has focused on square columns (Shamsai 2006) and retrofit of existing circular columns (Miller 2006). The purpose of this research project was to determine the characteristics of PCS reinforcement in circular columns, which to this point has not been investigated. Circular rebar reinforced columns, specifically those reinforced with spiral transverse reinforcement, have been shown through research to have superior confining abilities to rectangular columns. Researching the performance of PCS in circular columns allows for a better understanding of the confinement abilities of PCS.

To avoid buckling or other problems associated with slender columns, the test columns were designed with a 3:1 height to diameter ratio to ensure short column behavior. The test columns were designed to have a height of 18 in. and a diameter of 6 in.

For this research, the main focus was on the confining ability of the reinforcement, not the overall strength of the column. For this reason, the columns were lightly reinforced, with a longitudinal steel to concrete ratio (ρ) of 2 to 4%. This would allow the core concrete to carry the majority of the axial load, providing a more accurate understanding of the confinement abilities of each type of reinforcement.

For the rebar reinforced columns, it was decided that spiral reinforcement would be used. Spiral reinforcement has been shown through research to provide the greatest core confinement (Mander et al. 1988). Due to the light reinforcement of the columns, and the emphasis on confinement of core concrete, a #2 bar with a 1/4 in. diameter and a spiral spacing of 1.5 in. was selected as the transverse reinforcement. The 1.5 in. spacing is relatively small; however it will ensure that the core concrete is properly confined. The PCS columns will have a transverse reinforcement mechanism similar to circular ties instead of spiral ties, due to the fact that construction of PCS with transverse reinforcement modeled similarly to spiral ties would prove to be very difficult, expensive and impractical.

3.2 Test Parameters

The test parameters considered in this research project were the same as those considered in the research conducted by Shamsai (2006). These parameters included: the thickness of the reinforcement tube (t), width and length of the PCS openings (w) and (l) respectively, and height of the transverse reinforcement (h) as shown in Figure 3.1. However, for this research project, the two reinforcement systems, PCS and rebar, were not designed to have equivalent areas of steel, but equivalent yield forces, which is equal to the cross-sectional area of steel multiplied by the yield strength of the steel. This allowed for another parameter, yield strength, to be included in the research design.

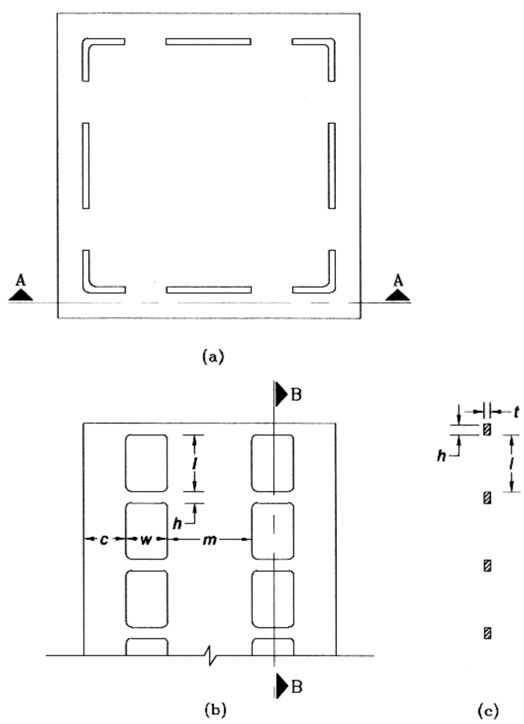

Figure 3.1 – Parameters used in PCS design: (a) plan section, (b) section A-A, (c) section B-B (Shamsai 2006)

3.2.1 Test Matrix

The test matrix consisted of two groups, Group 1 and Group 2. The only difference between the two groups was the size of the longitudinal rebar and the corresponding area of longitudinal steel. Group 1 consisted of three columns: a rebar column with a total of six #3 bars, for a total longitudinal steel area of 0.66 in.^{2}, and two PCS columns, one constructed from a 3/16 in. thick tube and another from a 1/4 in. thick tube. Group 2 also consisted of three columns: a rebar column with a total of six #4 bars, for a total longitudinal steel area of 1.2 in.^{2}, and two PCS columns, one constructed from a 3/16 in. thick tube and another from a 1/4 in. thick tube. Table 3.1 shows the test matrix and naming convention of the test columns.

Table 3.1 – Experimental test matrix with naming convention

Name	Group	Reinforcement	Tube Thickness	# bars	Opening Dim. (*w* x *l*)
1-RC-3	1	REBAR	#3 bar	6	--
1-PCS-.25	1	PCS	1/4" (.25 in.)	6	(1.974 x 1.330) in.
1-PCS-.188	1	PCS	3/16" (.188 in.)	6	(2.041 x 1.345) in.
2-RC-4	2	REBAR	#4 bar	6	--
2-PCS-.25	2	PCS	1/4" (.25 in.)	6	(1.645 x 1.330) in.
2-PCS-.188	2	PCS	3/16" (.188 in.)	6	(1.743 x 1.345) in.

3.2.2 Naming Convention

The naming convention used in this research project is fairly straight-forward, with the first number denoting which group the column is in, RC or PCS denoting the type of reinforcement used in the column, and the last number denoting the type of rebar used or the thickness of the steel tube used. For example, 1-PCS-.25 indicates a column in group 1 that is reinforced with PCS with a tube thickness of 0.25 in., as shown in Table 3.1.

3.3 Materials Used

The properties of the materials used in the construction of the columns are detailed in this section. All of the steel material properties were determined through testing according to ASTM standards in order to provide a more accurate understanding of each material's properties.

3.3.1 Concrete

The mix design selected for this research project is similar to the mix design of normal strength concrete used in M. Shamsai's PhD dissertation (2006). The concrete mix was designed to have an ultimate compressive strength of 4 ksi and a maximum aggregate size of 3/8 in., due to a clear cover spacing of only 1/2 in. Type III cement was used to allow for a more rapid strength gain, making it easier to remove the specimen from the formwork. To provide good workability, a slump within the range of 6-7 in. was selected. Table 3.2 shows the final mix design for this research project.

Table 3.2 – Concrete mix design

material	weight (lbs/batch)
water	76
cement	133
coarse aggregate	211
fine aggregate	294

According to Shamsai (2006), this mix design resulted in an average 28-day compressive strength of 4.85 ksi. As the columns have not yet been tested, the actual compressive strength of this mix design is not known. For theoretical modeling purposes, however, an ultimate compressive strength of 4.85 ksi is considered.

3.3.2 Steel Rebar

The steel rebar used in this research project is from the same batch as the rebar used by Miller (2006). Test coupons from each type of bar were obtained and tested in order to accurately obtain the properties of each steel bar. The steel test coupons were cut according to ASTM specifications. The coupons were then loaded under tension until fracture. An extensometer was used to record the strain in each test coupon. Figure 3.2 shows the rebar coupons used in the tension testing while Figure 3.3 shows the machine used to test the coupons.

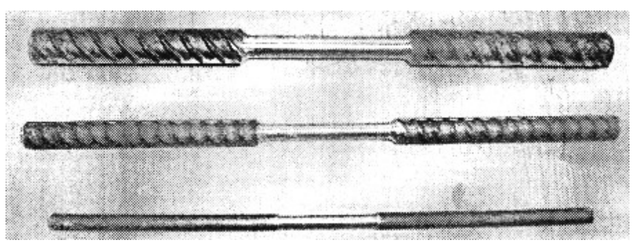

Figure 3.2 – Rebar test coupons (Miller 2006)

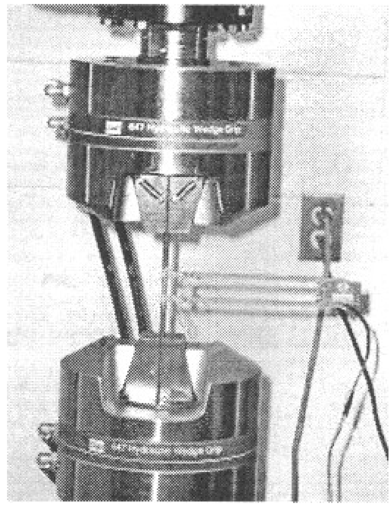

Figure 3.3 – Machine used to perform steel coupon testing (Miller 2006)

3.3.3 Steel Tubes

The steel tubes were tested in the same manner as the rebar. Test coupons were cut from the tubes according to ASTM standards. An example of one of the test coupons is shown in Figure 3.4 and a fractured coupon is shown in Figure 3.5.

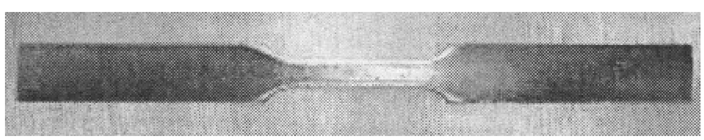

Figure 3.4 – Steel tube test coupon

The tube coupons were also loaded under tensile forces until failure, with the stress and corresponding strain values recorded in order to obtain an accurate plot of the material properties.

3.4 Column Design

As previously discussed, the columns were designed such that each column in a group would have the same steel yield force. The rebar columns were designed first, with the PCS dimensions being determined by the rebar properties. This section will describe how reinforcement for each column was designed.

3.4.1 Rebar

The rebar columns were designed to be lightly reinforced, as previously discussed in this chapter. The rebar columns consist of one column with six #3 bars as the longitudinal reinforcement and the other with six #4 bars as the longitudinal reinforcement. The rebar cage was designed to have an outside diameter of 5 in., allowing for 1/2 in. clear cover on all sides of the column, which has a 6 in. outside diameter. The rebar cage for 2-RC-4 is shown in Figure 3.6.

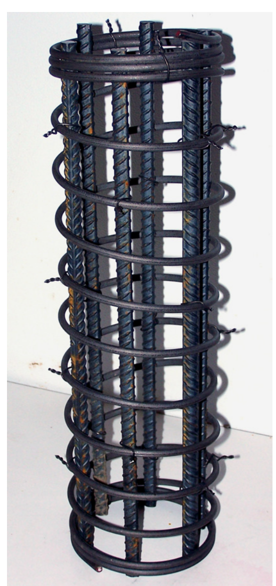

Figure 3.5 – Rebar cage for 2-RC-4

3.4.2 PCS

The design of the PCS columns was based on the properties of the rebar cages. The steel yield force in PCS can be varied by changing the size of the grid openings. The circular columns are more difficult to design than rectangular columns due to the curved surface. An Excel spreadsheet was constructed in order to calculate the dimensions of the windows in order to accurately match the steel yield force in the equivalent rebar column.

3.4.2.1 PCS 3-D

Initially, the PCS columns were modeled in a 3-D form. The tubes were laser-cut perpendicular to the curved surface. This allowed for an easy and accurate design, based on the percentage of the solid steel tube area of one steel strip. For design of the longitudinal strips, this percentage was then multiplied by 360 degrees in order to determine the angle required for the strip. This angle was subtracted from 60 degrees, for six total strips, in order to get the cut angle required. Since all six strips are identical, this angle was used for all six cuts, allowing for equal spacing between cuts. The design of the horizontal strips was much easier, as the cross-section was just a simple rectangle. The height of the strips was found by dividing the yield force of the #2 rebar by the yield strength of the tube and the thickness of the tube. The spacing used in the rebar columns, 1.5 in., was also used in the PCS columns. The window height was calculated by subtracting the height of one strip from 1.5 in. The one problem associated with 3-D cutting is its high cost. Because of this, a different method was examined.

3.4.2.1 PCS 2-D

In order to reduce costs associated with laser-cutting, a 2-D method of production was examined due to the fact that 2-D laser-cutting is less expensive than 3-D. The design of the transverse steel was the same as the 3-D method, because the curve of the tube has no bearing on this design. The design of the longitudinal strips was where the change was. Figure 3.5 shows a sketch of the 2-D design.

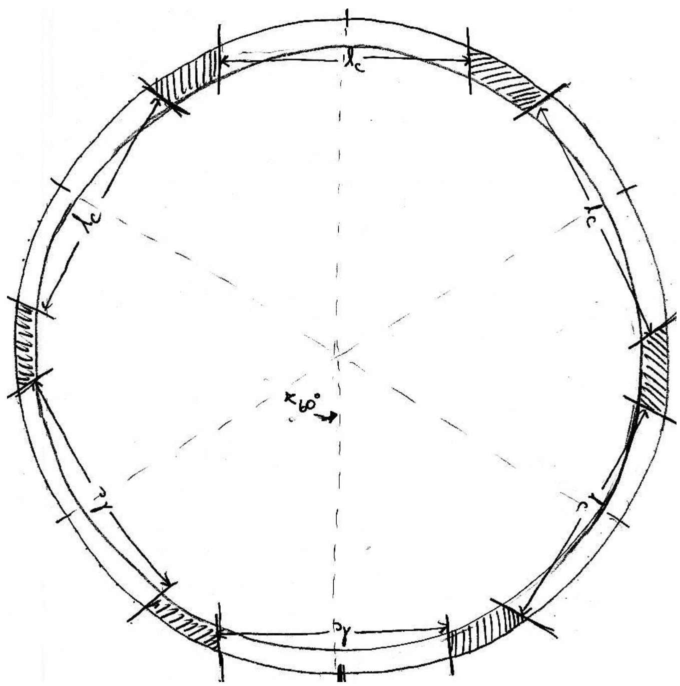

Figure 3.6 – 2-D design for longitudinal PCS strips

The design was based off of the initial 3-D design. The difference between the vertical and perpendicular cuts was small due to the thin walled tubes, but not small enough to be completely disregarded. The steel area was calculated to be the area of the strips based on a cut perpendicular to the surface minus the small fraction of area cut off by the horizontal cuts. This total area was set equal to the required area, and the resulting dimension, l_c, was calculated through an iterative process. The result was a design that was not too different from the 3-D design, but with the potential to be less expensive to manufacture.

3.5 Column Construction

Once the PCS is manufactured, the columns will be cast. The formwork for the columns consists of cardboard tubes that are 18 in. tall with a 6 in. inside diameter. The formwork will be lined with packing tape and coated with WD-40 before casting the columns to allow for easier removal of the columns from their formwork. Once cast, the columns will be kept hydrated in order to prevent poor curing and a possible loss of strength. Two days after casting, the columns will be removed from their formwork and allowed to cure in a water bath. This will increase the initial strength of the columns and also provide better overall curing. The concrete mix used in the construction of the columns is described in Section 3.3.1.

CHAPTER 4

COLUMN THEORETICAL MODELS

4.1 Introduction

The next part of this research project involved using the models proposed by Mander et al. (1988) and Hoshikuma et al. (1997) in conjunction with the material properties described in Chapter 3 in order to theoretically predict the behavior of each test column. These theoretical models will then be compared to the actual test results in order to determine the appropriateness of the selected models for concrete in the test columns, specifically the PCS reinforced columns. Due to the monolithic construction of PCS, along with its other differences compared to rebar reinforcement, the axial load-deflection plot for PCS columns may not be the same as the rebar columns. Previous research conducted by Shamsai (2006), involving square PCS columns, found that the PCS fractured at the joint where the transverse strips met the longitudinal strips, as shown in Figure 4.1. Previous research conducted by Miller (2006), involving circular columns retrofit with PCS, found that a number of fractures happened diagonally through the joint of the longitudinal and transverse steel strips. This is shown in Figure 4.2 below.

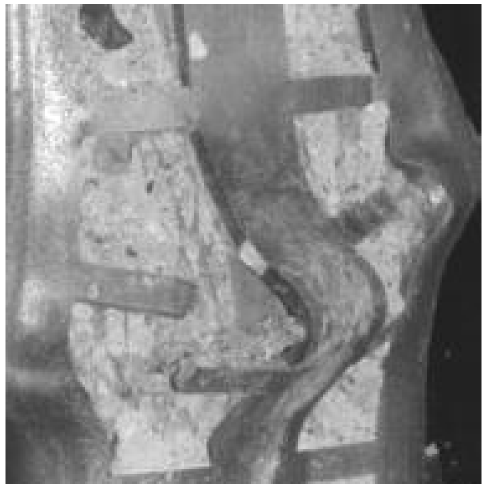

Figure 4.1 – Failure of square PCS columns (Shamsai 2006)

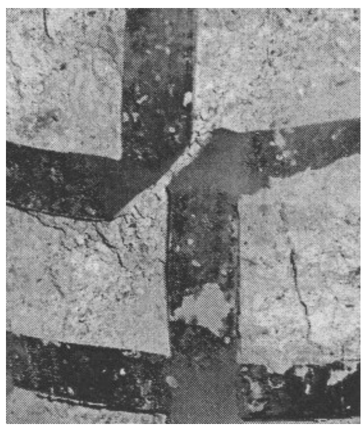

Figure 4.2 – Failure of circular PCS retrofit column (Miller 2006)

These images show the different forms of failure in PCS columns. These failures are not identical to that of a rebar column, especially the diagonal fracture, in which one of the transverse bars fractures. This difference is due mainly to the monolithic construction of PCS. The result is a column that may perform differently than a rebar column under axial load. The models presented in the following chapter will be compared to the obtained test data to determine the validity of the current models to PCS and may help to develop a more accurate model for PCS columns.

4.2 Material Properties

In the following section, the stress-strain plots for each material used in the construction of the columns will be presented. Then, in Section 4.3, these material properties will be used to construct the theoretical models for each column.

4.2.1 Concrete

Based on the mix design discussed in Chapter 3, the expected ultimate strength of the plain concrete is 4.85 ksi after 28 days. The stress-strain plot for this concrete can be modeled through the use of Mander et al.'s model for concrete strength, defined by Equation 2.1. The only changes are that f'_{cc} is replaced with f'_{co}, and ε_{cc} is replaced with ε_{co}, with ε_{co} taken as 0.002. The resulting model for 4.85 ksi concrete is shown in Figure 4.3.

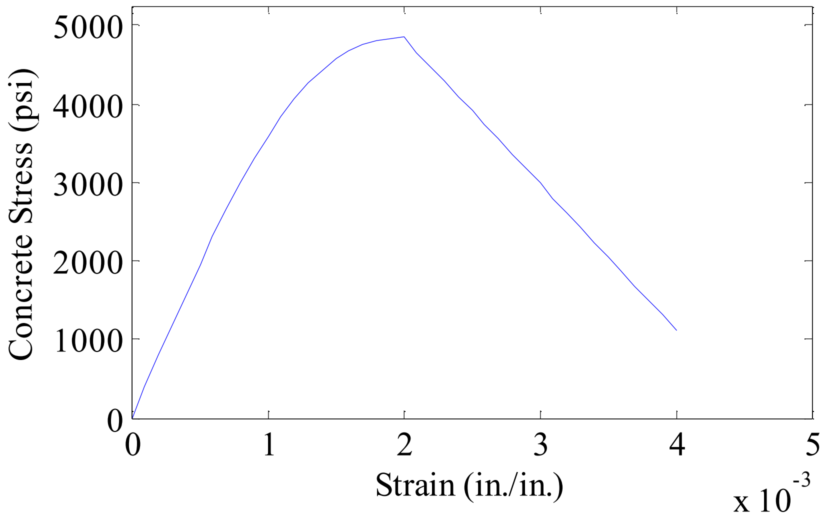

Figure 4.3 – Theoretical stress-strain plot for plain concrete

4.2.2 Steel Rebar

Three different types of rebar were used: #2 bar (1/4 in. diameter), #3 bar (3/8 in. diameter) and #4 bar (1/2 in. diameter). Each bar type had different characteristics as far as its stress-strain behavior, due to the steel material differences. In order to model the steel behavior, the stress-strain curve was broken into three sections consisting of three different equations. The first section was the elastic section, in which the steel behavior is defined as the strain multiplied by the modulus of elasticity of steel, shown in Equation 4.2. For the steel used in this research project, the modulus of elasticity was assumed to be 29,000 ksi.

$$f_s = E_s \varepsilon_s \qquad 4.2$$

Along the yield plateau, the stress is modeled as a straight line between the yield point and the onset of strain hardening. The stress at which strain hardening starts is denoted as f_{sh}, while the strain at the onset of strain hardening is denoted as ε_{sh}. This linear behavior is defined by Equation 4.3.

$$f_s = \left[\frac{\left(f_{sh} - f_y\right)}{\left(\varepsilon_{sh} - \varepsilon_y\right)}\right]\varepsilon_s + \left[f_y - \frac{\varepsilon_y\left(f_{sh} - f_y\right)}{\left(\varepsilon_{sh} - \varepsilon_y\right)}\right] \qquad 4.3$$

The final phase, strain hardening through eventual necking and failure, is defined through a parabolic equation defined in Equation 4.4. The ultimate stress of the steel is denoted as f_u while the ultimate strain is denoted as ε_{su}.

$$f_s = f_u - \left(f_u - f_{sh}\right)\left[\frac{\varepsilon_{su} - \varepsilon_s}{\varepsilon_{su} - \varepsilon_{sh}}\right]^2 \qquad 4.4$$

Through the use of these three equations, a theoretical stress-strain plot for each rebar size was created and plotted along side of the measured data in order to determine the accuracy of the model. The plots for the #2, #3 and #4 rebars are given in Figures 4.4, 4.5 and 4.6, respectively.

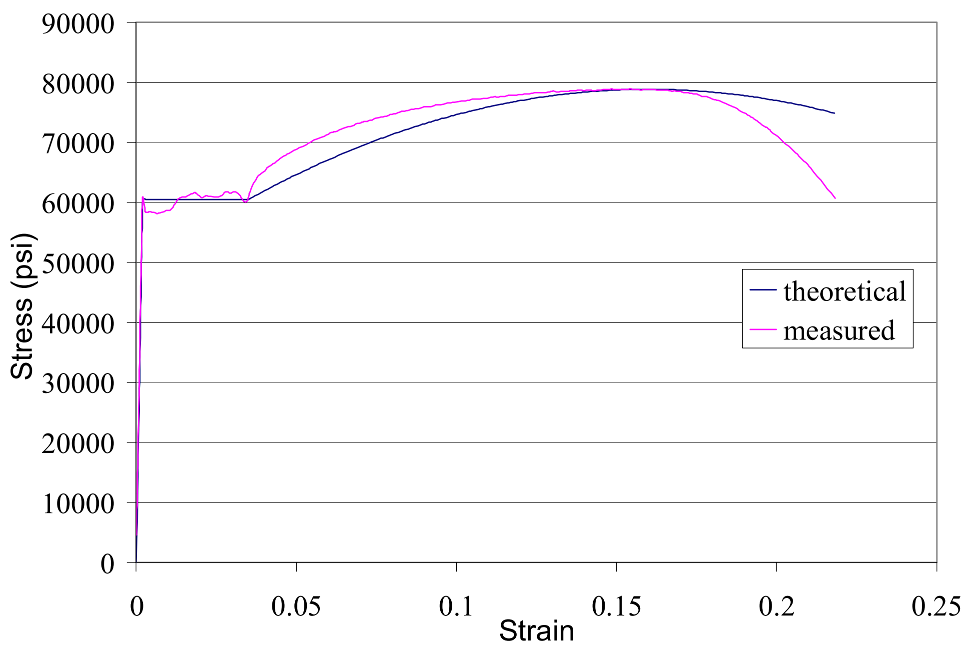

Figure 4.4 – Theoretical vs. actual stress-strain plot for #2 rebar

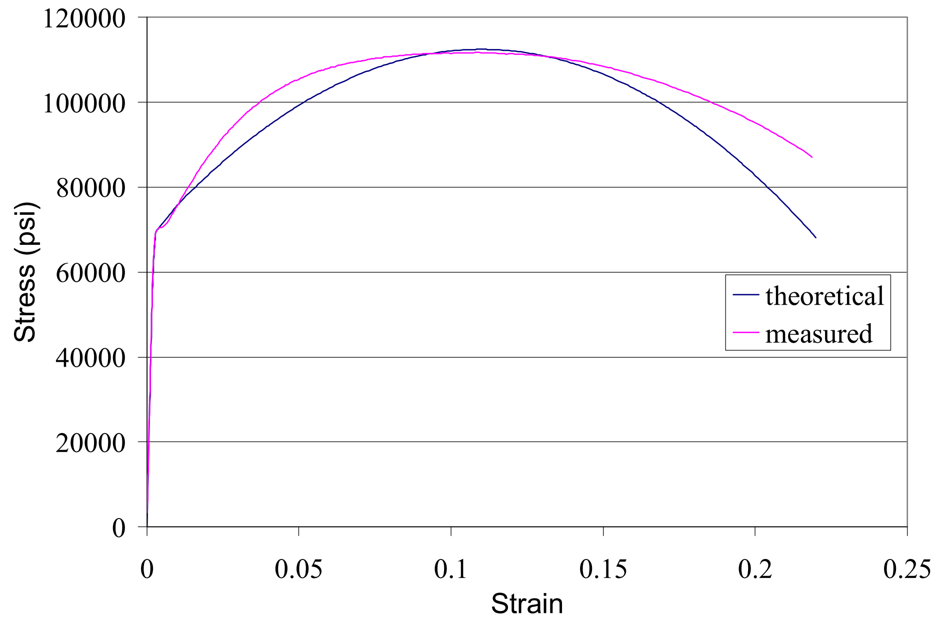

Figure 4.5 – Theoretical vs. actual stress-strain plot for #3 rebar

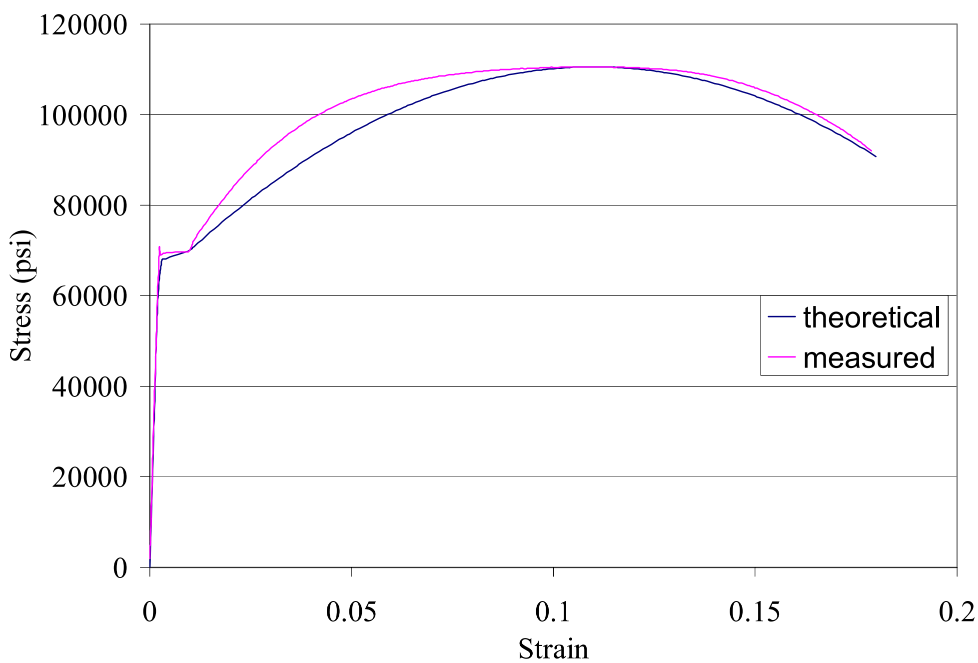

Figure 4.6 - Theoretical vs. actual stress-strain plot for #4 rebar

As shown in the plots, the theoretical models closely resemble the actual material properties, which will allow for a more accurate column model.

4.2.3 Steel Tubes

Steel tubes with an outside diameter of 5 in. were used in this research project. Two different wall thicknesses were used, 1/4 in. and 3/16 in. The two tube thicknesses were expected to have similar yield strengths; however tension testing showed this to not be the case. The 3/16 in. thick tubes have a considerably higher yield strength, 90 ksi, than the 1/4 in. thick tubes, at 67 ksi. This is due, most likely, to the different tubes being from two entirely different batches, although the manufacturer stated that they were of similar properties. Because the dimensions for PCS are based on steel yield force, not just area of steel, the differences caused by the different yield strengths of the tubes should not have too great of an effect on the overall performance of the test columns. It will also allow for some basic comparisons between the performance of high yield strength-less ductile steel and lower yield strength-higher ductility steel. The theoretical stress-strain models for the steel tubes were developed in the same manner as the rebar models, through the use of Equations 4.2 through 4.4. The models were then plotted along with the measured data in order to determine the accuracy of the models. These plots are shown in Figures 4.7 and 4.8 for the 3/16 in. and 1/4 in. thick tubes, respectively.

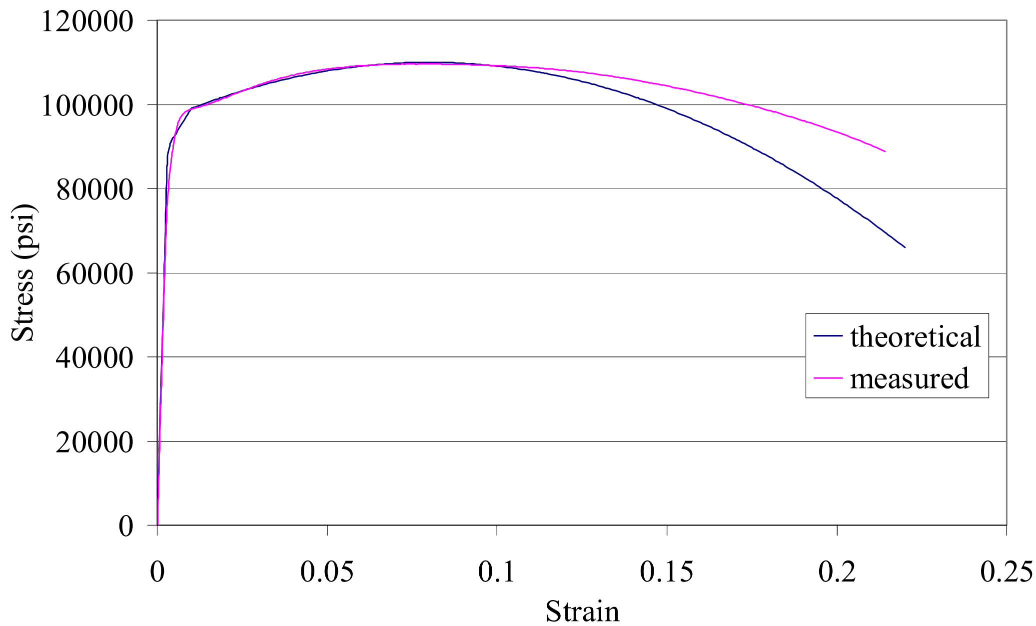

Figure 4.7 - Theoretical vs. actual stress-strain plot for 3/16 in. thick tube

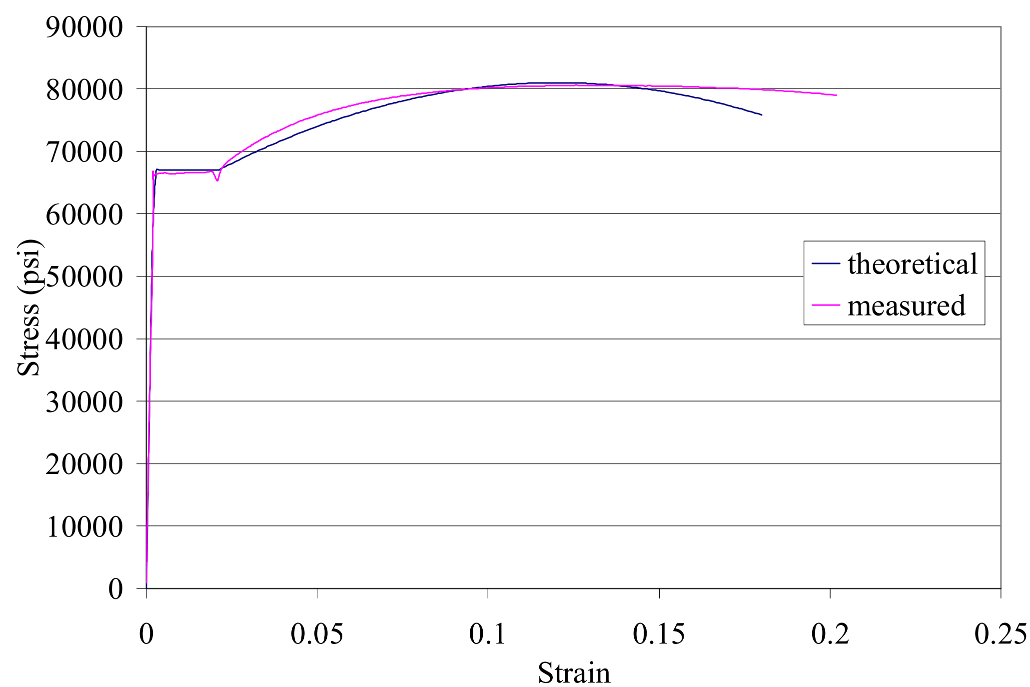

Figure 4.8 - Theoretical vs. actual stress-strain plot for 1/4 in. thick tube

4.3 Column Theoretical Models

The axial load-deflection models for the test columns were constructed using the theoretical models of the materials. The equations used to model the columns were based on the general equations for calculating the axial capacity, P, of a column. There are a total of two equations used, one equation to calculate the axial load before the cover concrete spalls off (Equation 4.5), and the other to calculate the axial load after spalling of the cover concrete (Equation 4.6).

$$P = f_c\left(A_g - A_{st}\right) + f_s\left(A_s\right) \qquad 4.5$$

$$P = f_c\left(A_e\right) + f_s\left(A_s\right) \qquad 4.6$$

The variable A_e stands for the effectively confined concrete core after spalling and arching. The equation for A_e given by Mander et al. (1988) is adapted.

$$A_e = \frac{\pi}{4}\left(d_s - \frac{s'}{2}\right)^2 \qquad 4.7$$

4.3.1 Columns in Group 1

Included in this section are the theoretical axial load-deflection plots for the columns in Group 1. Each plot was constructed using the models proposed by Mander et al. (1988) and Hoshikuma et al. (1997), found in Chapter 2 of this report. The models of each column are fairly similar, due to the design constraints in which the steel yield force in each group was held constant. Due to material imperfections and the broad nature of the proposed models, it is expected that the performance of the test columns will not follow exactly with the theoretical models. The models instead serve as a control in the experiment, providing a base on which to compare the overall performance of the test columns.

4.3.1.1 Column 1-RC-3

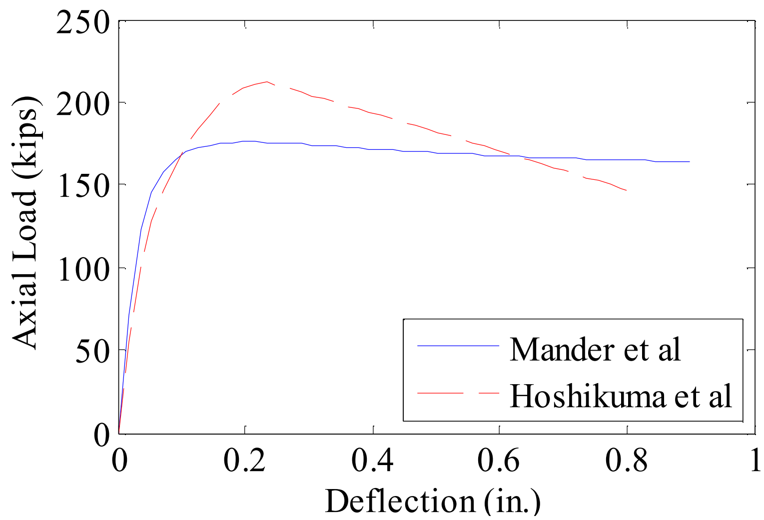

Figure 4.9 – Axial load-deflection plot for 1-RC-3

4.3.1.2 Column 1-PCS-.188

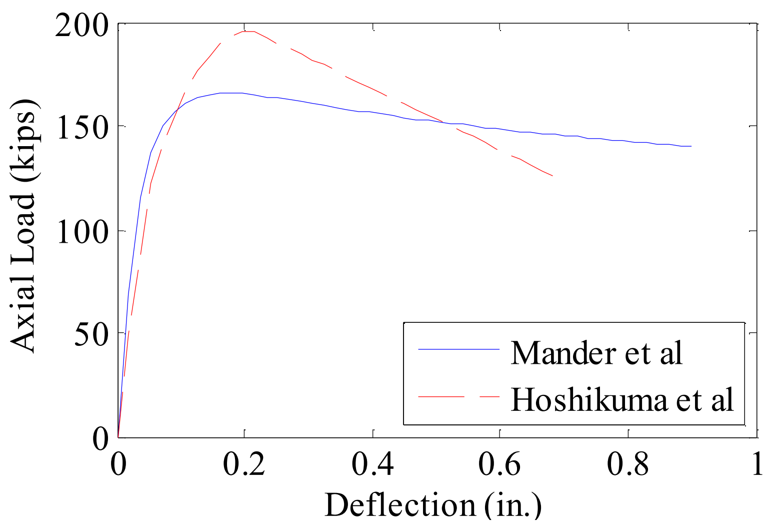

Figure 4.10 – Axial load-deflection plot for 1-PCS-.188

4.3.1.3 Column 1-PCS-.25

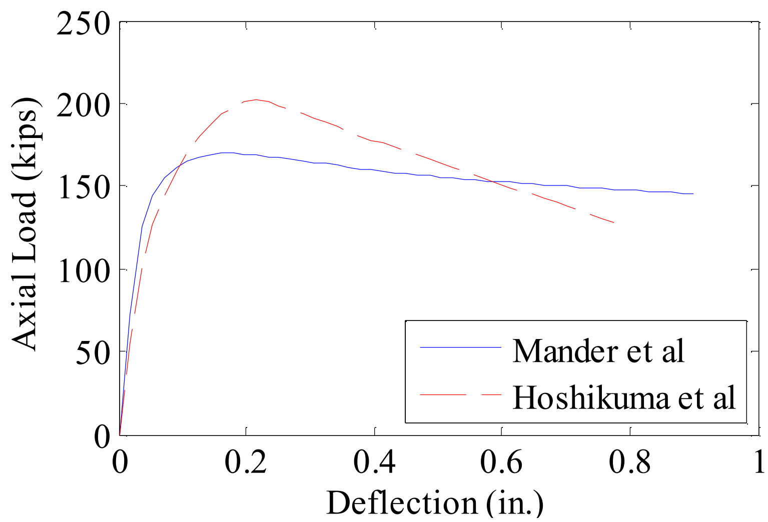

Figure 4.11 – Axial load-deflection plot for 1-PCS-.25

4.3.2 Group 2

Included below are the theoretical models for Group 2 constructed using Mander et al.'s (1988) model and Hoshikuma et al.'s (1997) model for confined concrete. The columns in Group 2 showed a greater ultimate compressive strength than those in Group 1, due to an increase in the longitudinal steel area of almost 100%.

4.3.2.1 Column 2-RC-4

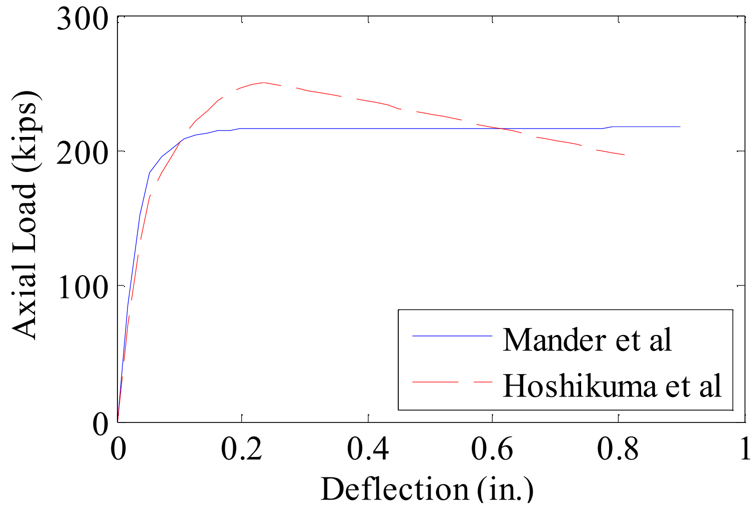

Figure 4.12 – Axial load-deflection plot for 2-RC-4

4.3.2.2 Column 2-PCS-.188

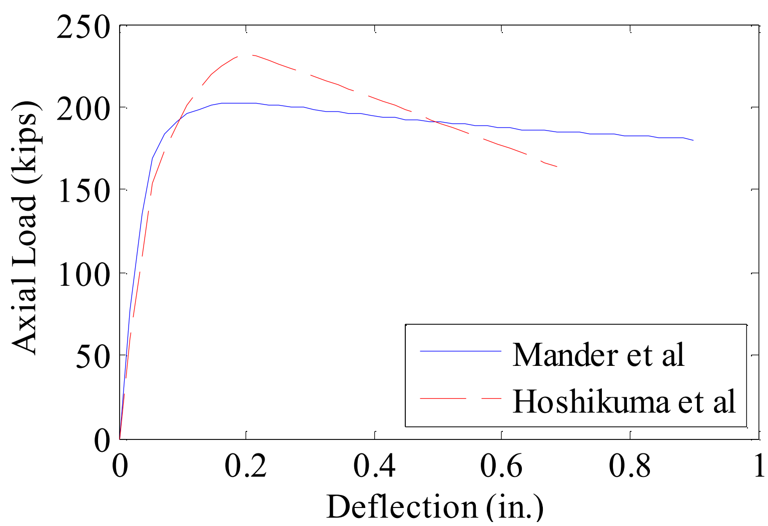

Figure 4.13 – Axial load-deflection plot for 2-PCS-.188

4.3.2.3 Column 2-PCS-.25

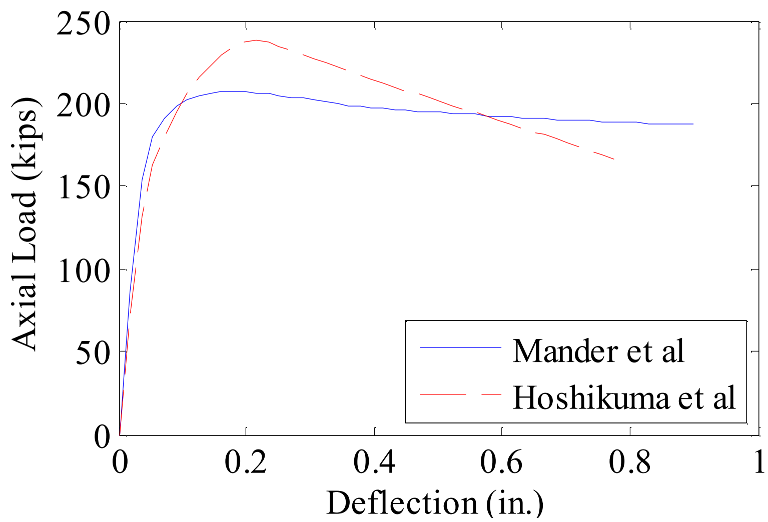

Figure 4.14 – Axial load-deflection plot for 2-PCS-.25

4.4 Theoretical Comparisons

In order to better compare the different columns within each group, the individual curves were plotted together. The two different models were separated, in order to avoid having too much data in one plot. The plots are included as Figures 4.15 and 4.16 for group 1, and Figures 4.17 and 4.18 for Group 2.

4.4.1 Group 1

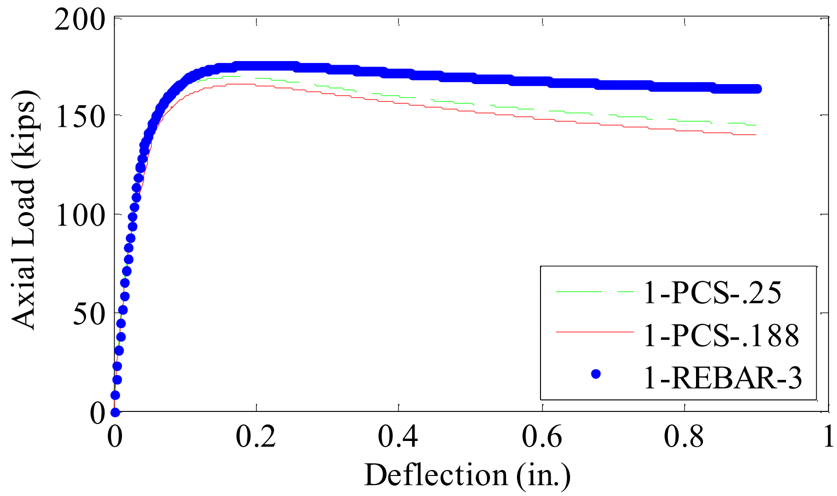

Figure 4.15 – Axial load-deflection curves for Group 1 using Mander et al.'s model

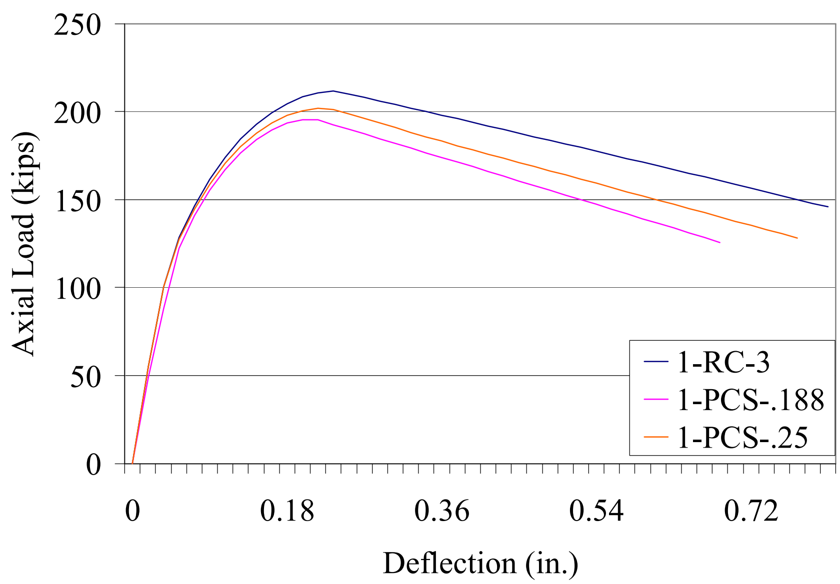

Figure 4.16 – Axial load-deflection curves for Group 1 using Hoshikuma et al.'s model

4.4.2 Group 2

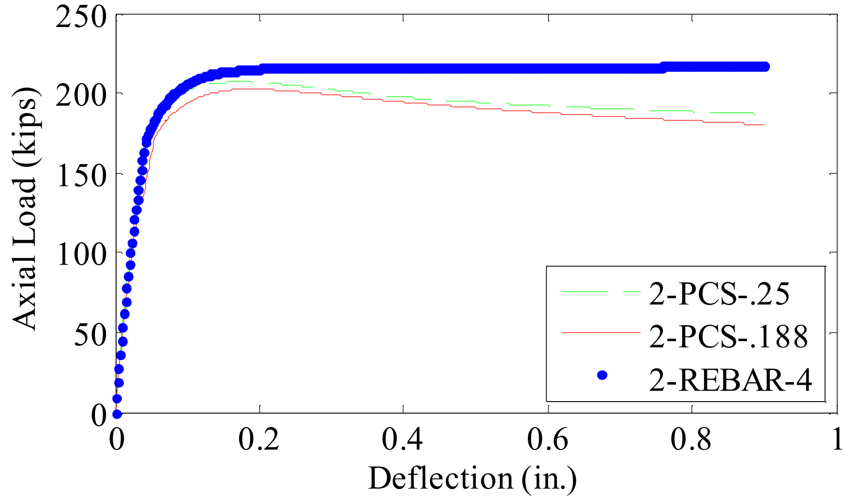

Figure 4.17 – Axial load-deflection curves for Group 2 using Mander et al.'s model

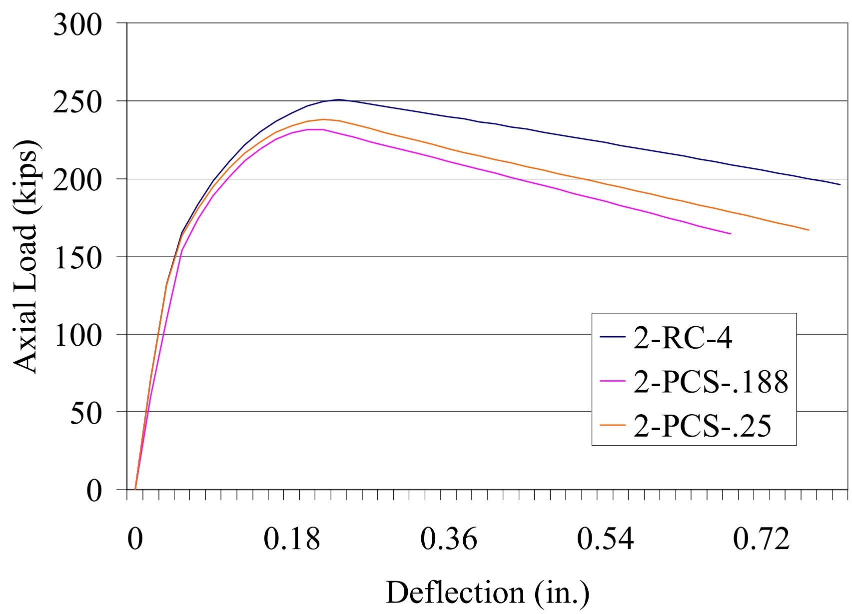

Figure 4.18 – Axial load-deflection curves for Group 2 using Hoshikuma et al.'s model

CHAPTER 5

CONCLUSIONS

5.1 Project Summary

A test matrix was developed for the purpose of comparing a recently proposed alternative of steel reinforcement, PCS, to the existing standard form of steel reinforcement used in concrete columns, rebar cages. A total of six specimens were to be tested, divided into two groups. Within each group, the yield force in each column was kept the same in order to account for the differences in material properties between the different types of steel used. However, the yield force was different between the two groups. This allowed for an accurate comparison between members in each group, while also allowing for an opportunity to gage the effect of the amount of steel present on the overall effectiveness of the PCS reinforcement. Each group consisted of one rebar column to serve as the control and two PCS columns with different wall thicknesses but identical yield forces.

The steel materials used in this research project were all tested according to ASTM standards to obtain an accurate understanding of each material's mechanical properties.

The concrete and steel material properties were used to construct theoretical models for each test column, according to the methods proposed by Mander et al. (1988) and Hoshikuma et al. (1997). The models were then analyzed and compared within their respected groups to gain a better understanding of each test column. The next step will be to construct and test the columns and compare the actual performance to the predicted performance of the models.

5.2 Steel Reinforcement Methods

In Section 4.4, the predicted behavior of each column is compared to the other columns in its group. For both groups, the rebar column had a slightly higher axial strength and showed higher ductility, demonstrated by the more gradual decline of the axial load-deflection curve. However, the predicted ultimate load and ductility of the PCS columns was not much less than the rebar columns. Also, the models used do not consider the possibility of increased confinement provided by PCS. These differences in the theoretical models will allow for a better comparison between the actual axial load-deflection curves of the test columns. The differences in the actual curves can be compared to determine if they are less or greater than the theoretical curves, allowing for a good comparison between the actual confinement abilities of the transverse reinforcement used in the rebar and PCS columns.

5.3 Future of Project

The actual test columns must still be constructed and tested for this project to be successful. The materials are all obtained and the designs have been finished. The next step in this research project is the laser-cutting of the steel tubes. Once the PCS reinforcement is ready, the columns will be cast and allowed to cure for 28 days. Once the columns have reached their 28-day strength, they will be tested under constant axial load until failure. The test data that is obtained will be compared to the theoretical data presented in this thesis in order to gain a better understanding of the performance of PCS and its relationship to the standard method of reinforcement, steel rebar.

LIST OF REFERENCES

Hoshikuma, J., Kawashima, K., & Taylor, A.W. (1997). Stress-strain model for confined concrete in bridge piers. *Journal of Structural Engineering*, 123(5), 624-633.

Mander, J.B., Priestly, M.J.N., & Park, R. (1988). Theoretical stress-strain model for confined concrete. *Journal of Structural Engineering*, 114(8), 1804-1826.

Mander, J.B., Priestly, M.J.N., & Park, R. (1988). Observed stress-strain behavior of confined concrete. *Journal of Structural Engineering*, 114(8), 1827-1849.

Miller, E. (2006). Experimental research of reinforced concrete column retrofit methods. Unpublished master's thesis, The Ohio State University, Columbus.

Popovics, S. (1973). A numerical approach to the complete stress-strain curve of concrete. *Cement and Concrete Research*, 3(5), 583-599.

Shamsai, M. (2006). Experimental analysis of pre-fabricated cage system (PCS) reinforcement. Unpublished doctoral dissertation, The Ohio State University, Columbus.